

<https://doi.org/10.1038/s41514-025-00321-1>

MicroRNA profiles in plasma-derived extracellular vesicles across the human lifespan

Check for updates

C. Ráez-Meseguer^{1,2,3}, C. Navas-Enamorado⁴, X. Capó^{3,4}, AM Galmes-Panades^{5,6}, A. Molina de la Llave⁴, M. Mendez-Varela⁴, M. Martínez-Calvo⁴, A. Bennasar-Arbois⁴, A. Sánchez-Polo⁴, L. Masmiquel⁷, M. Torrens-Mas^{2,8}, M. Monjo^{1,2,3}, JM Ramis^{1,2,3} ✉ & M. Gonzalez-Freire⁴ ✉

Extracellular vesicles (EVs) are key mediators of intercellular communication and may reflect physiological changes during aging. We analyzed plasma-derived EVs from a healthy aging cohort stratified by age, using size exclusion chromatography, surface profiling, nanoparticle tracking, and small RNA sequencing. While EV size and concentration remained largely unchanged, older individuals showed shifts in EV immunophenotype consistent with immunosenescence and displayed distinct miRNA signatures enriched in muscle-specific and metabolism-related miRNAs, including miR-206, miR-143-3p, miR-122-5p, and miR-20b-3p—linked to muscle, metabolic, and vascular function. Notably, miR-6529-5p, associated with neuroprotection, was elevated in aging. Target gene analysis revealed involvement in aging pathways such as Ras, VEGF, and MAPK signaling. EV miRNAs and particle counts correlated with biological aging markers, including GDF-15, visceral fat, and muscle quality. These findings highlight coordinated age-related changes in EVs reflecting musculoskeletal and metabolic aging and support their potential as minimally invasive biomarkers of biological aging and functional decline.

Aging is a complex and multifactorial process characterized by the progressive accumulation of cellular and molecular damage over time, ultimately leading to a decline in physiological function, increased susceptibility to chronic diseases, and impaired cognitive and social capacities^{1,2}. Understanding the molecular underpinnings of aging is essential to identifying early biomarkers and potential therapeutic targets that may preserve healthspan and delay the onset of age-related decline^{3,4}. Among the biological systems currently under investigation, extracellular vesicles (EVs) have emerged as promising mediators and biomarkers of aging. EVs are membrane-bound nanoscale particles released by virtually all cell types and play a critical role in intercellular communication by transporting molecular cargo—such as proteins, lipids, and RNAs—that reflect the physiological status of their cells of origin^{5–7}. Their composition, secretion patterns, and molecular content, including

non-coding RNAs, can vary with age and cellular stress, offering a window into systemic physiological changes^{8,9}.

One of the most studied classes of EV cargo is microRNAs (miRNAs)—short, non-coding RNA molecules approximately 22 nucleotides in length. miRNAs act as key regulators of gene expression, often through the repression of target mRNAs, and are involved in fundamental biological processes such as development, immune response, metabolic regulation, and stress adaptation^{10–12}. miRNAs can be encapsulated within EVs, where they remain protected and stable in circulation, allowing them to mediate long-distance cell-to-cell signaling¹³. Importantly, several miRNAs have been implicated in several hallmarks of aging, including oxidative stress, mitochondrial dysfunction, cellular senescence, and chronic inflammation^{14–18}. Recent studies suggest that both the quantity and molecular composition of circulating EVs change with age^{19–21}. Notably,

¹Group of Cell Therapy and Tissue Engineering (TERCIT, Research Institute on Health Sciences (IUNICS), University of the Balearic Islands, Palma, Spain. ²Health Research Institute of the Balearic Islands (IdISBa), Palma, Spain. ³Department of Fundamental Biology and Health Sciences, University of the Balearic Islands, Palma, Spain. ⁴Translational Research in Aging and Longevity (TRIAL) Group, Health Research Institute of the Balearic Islands (IdISBa), Palma, Spain. ⁵Physical Activity and Sport Sciences Research Group (GICAFE), Institute for Educational Research and Innovation (IRIE), University of the Balearic Islands, Palma, Spain. ⁶Consorcio CIBER, M.P. Fisiopatología de la Obesidad y Nutrición (CIBEROBn), Instituto de Salud Carlos III (ISCIII), Madrid, Spain. ⁷Vascular and Metabolic Pathologies Group, Health Research Institute of the Balearic Islands (IdISBa), Palma, Spain. ⁸Grupo Multidisciplinar de Oncología Traslacional, Research Institute on Health Sciences (IUNICS), University of the Balearic Islands, Palma, Spain. ✉e-mail: joana.ramis@uib.es; martagonzalezfreire@gmail.com

EVs secreted by senescent cells have been shown to propagate senescence-associated signals and contribute to the development of age-related pathologies^{22,23}. However, to establish EVs as reliable biomarkers of aging, it is necessary to comprehensively characterize their abundance, molecular content, and functional signatures across the lifespan^{24,25}. In particular, age-related differences in EV-associated miRNA profiles remain incompletely understood.

In this study, we sought to characterize the plasma-derived EVs and their small RNA cargo across a cohort of healthy individuals ranging from 20 to over 80 years of age. We combined EV surface profiling, nanoparticle tracking analysis, and small RNA sequencing to assess age-dependent changes in EV abundance, size, and molecular content. Given the central role of skeletal muscle in metabolic health and functional capacity, and its particular vulnerability to aging, we placed special emphasis on identifying miRNA signatures related to musculoskeletal function.

Results

Characterization of plasma-derived extracellular vesicles

Summarized epidemiological data of the participants are presented in Table 1 (by sex) and Table 2 (by age group). Plasma-derived EVs were isolated using size exclusion chromatography from three age groups: young ($n = 12$), middle-aged ($n = 13$), and old ($n = 14$). EV surface profiling was carried out using the MACSPlex Exosome Kit, which enables the detection of 37 surface-associated proteins per group, including classical exosomal markers CD9, CD63, and CD81 (Fig. 1A). A heatmap of normalized mean fluorescence intensities revealed age-dependent variations in EV surface protein composition. Specifically, a progressive decrease in CD3, CD56 (neural cell adhesion molecule), HLA-A (MHC class I), and CD45 (pan-leukocyte marker) expression was observed with advancing age. CD14 and CD69

showed a trend toward an increase in the older group, though these differences should be interpreted cautiously, given the pooled nature of the samples. Nanoparticle tracking analysis (NTA) was used to quantify EV concentration and size distribution across the full cohort ($n = 39$) (Fig. 1B, C). No statistically significant differences were found in EV concentration or mean particle size according to age or sex. Potential outliers were evaluated using the interquartile range (IQR) method (values $> 1.5 \times$ IQR beyond quartiles). One individual in the older group showed EV concentration $> 3 \times$ IQR above the third quartile. However, this value was retained in analyses as it represented a biologically plausible measurement with consistent quality control metrics, and its removal did not substantially alter the statistical conclusions (trend remained: $p = 0.15$ with outlier vs. $p = 0.22$ without). A trend toward increased EV concentration with age was noted, suggesting possible age-related alterations in vesicle release or clearance dynamics. When examined as a continuous variable, chronological age showed a modest positive association with EV concentration ($r = 0.32$, $p = 0.05$), indicating a gradual increase in EV release across the adult lifespan (Supplementary Fig. 2). In contrast, EV particle size did not display a significant relationship with age ($r = -0.22$, $p = 0.18$; Supplementary Fig. S5B). These continuous-age analyses support the trends observed in the categorical comparisons, reinforcing that EV concentration tends to rise with advancing age, whereas EV size remains largely stable.

Age-related differences in EV-associated small RNAs

Small RNA sequencing of plasma-derived EVs was conducted to investigate age-dependent molecular signatures. Annotation of the EV-associated RNA reads followed a hierarchical prioritization (known miRNA $>$ rRNA $>$ tRNA $>$ snRNA $>$ snoRNA $>$ repeat $>$ gene $>$ novel miRNA). A total of 762 miRNAs were identified in plasma-derived extracellular vesicles, including

Table 1 | Baseline characteristics of the 39 participants included in the study

	Total ($n = 39$)	Male ($n = 21$)	Female ($n = 19$)	p
Age (years)	48.5 (20–85) \pm 2.8	49.3 (23–79) \pm 3.9	47.6 (20–85) \pm 4.3	0.767
Sex (female)	19 (49%)	–	–	
Height (m)	1.69 (1.47–1.87) \pm 0.01	1.77 (1.61–1.87) \pm 0.01	1.61 (1.47–1.69) \pm 0.01	<0.001*
Weight (kg)	69.7 (44.5–100) \pm 2.27	78.2 (58.8–100) \pm 2.6	58.6 (44.5–77.2) \pm 2.0	<0.001*
Body mass index (kg/m ²)	23.8 (17.3–35.7) \pm 0.6	25.1 (19.4–30.8) \pm 0.7	22.5 (17.3–35.7) \pm 0.9	0.025*
Basal metabolic rate	1517 (1095–2130) \pm 45.8	1738 (1297–2130) \pm 47.1	1284 (1095–1500) \pm 27	<0.001*
Body fat mass (kg)	16.0 (5.8–39.1) \pm 1.1	15.6 (5.8–31.5) \pm 1.4	16.3 (7.4–39.1) \pm 1.8	0.776
Soft lean mass (kg)	49.6 (31.4–77.1) \pm 2.0	58.9 (40.5–77.1) \pm 2.0	39.8 (31.4–49.3) \pm 1.2	<0.001*
Fat-free mass	52.7 (33.6–81.5) \pm 10.6	62.5 (42.9–81.5) \pm 2.1	42.3 (33.6–52.3) \pm 1.3	<0.001*
Visceral fat area	75.1 (22.2–202.8) \pm 6.4	72.7 (22.2–156.8) \pm 7.7	77.6 (27.7–202.8) \pm 10.6	0.708
Waist-hip ratio	0.900 (0.900–1.09) \pm 0.010	0.910 (0.790–1.08) \pm 0.020	0.880 (0.790–1.09) \pm 0.020	0.393
50 kHz body phase angle	5.53 (3.60–6.70) \pm 0.13	5.90 (3.60–6.70) \pm 0.17	5.16 (3.90–6.20) \pm 0.15	0.004*
Physical performance				
Grip Strength (kg/cm)	30.6 (10.5–53.4) \pm 1.8	39.4 (27.5–53.4) \pm 1.5	21.4 (10.5–35.9) \pm 1.5	<0.001*
Chair Test (s)	9.40 (5.30–20.7) \pm 0.50	9.40 (6.40–20.7) \pm 0.70	9.40 (5.30–15.93) \pm 0.60	0.949
Walking speed (normal) (s)	3.50 (2.23–4.43) \pm 0.07	3.50 (2.76–4.43) \pm 0.10	3.50 (2.23–4.06) \pm 0.10	0.748
Walking speed (fast) (s)	2.23 (0.72–3.28) \pm 0.07	2.10 (0.72–3.00) \pm 0.09	2.40 (1.80–3.28) \pm 0.09	0.016*
Inflammatory markers				
GDF-15	446 (131–1335) \pm 40	465 (131–1335) \pm 63	428 (219–1011) \pm 50	0.646
Exosomes characterization				
Extracellular vesicles number (particles/mL)	4.99×10^8 (1.34×10^7 – 5.95×10^9) \pm 1.75×10^8	6.29×10^8 (1.34×10^7 – 5.95×10^9) \pm 2.94×10^8	3.61×10^8 (2.21×10^7 – 3.70×10^9) \pm 1.87×10^8	0.452
Extracellular vesicles size (nm)	139 (110–175) \pm 3	136 (110–162) \pm 3	143 (112–175) \pm 4.0	0.134

Data are mean \pm (SEM), range () or %.

*Statistically significant ($p < 0.05$).

Table 2 | Baseline characteristics of the 39 participants included in the study

	Young (n = 12)	Middle age (n = 13)	Old (n = 14)	p
Age (years)	27.4 (20–33) ± 1.3	47.1 (39–56) ± 1.50 [†]	68.8 (60–85) ± 2.2 ^{*,#}	<0.001*
Sex (female)	6 (15.4%)	6 (15.4%)	7 (17.9%)	
Height (m)	1.71 (1.53–1.83) ± 0.02	1.71 (1.57–1.87) ± 0.02	1.66 (1.47–1.85) ± 0.03	0.584
Weight (kg)	69.3 (44.5–91.9) ± 4.6	65.4 (48.3–85.6) ± 3.1	71.1 (48.6–100) ± 4.1	0.239
Body composition				
Body mass index (kg/m ²)	23.3 (17.3–28.7) ± 1.0	22.4 (19.4–28) ± 0.7	25.7 (21.3–35.7) ± 0.6	0.042
Basal metabolic rate	1615 (1126–1964) ± 93	1529 (1209–1854) ± 59	1422 (1095–2130) ± 81	0.232
Body fat mass (kg)	13.2 (7.40–18.3) ± 1.1	11.8 (5.80–22.3) ± 1.2	22.3 (15.0–39.1) ± 1.8 ^{*,#}	<0.001*
Soft lean mass (kg)	52.8 (32.8–69.6) ± 3.9	50.6 (36.5–64.7) ± 2.6	45.9 (31.4–77.1) ± 3.6	0.329
Fat-free mass	56.1 (35.0–73.8) ± 4.1	53.7 (38.8–68.7) ± 2.7	48.7 (33.6–81.5) ± 3.7	0.326
Visceral fat area	56.7 (28.0–79.9) ± 5.2	52.2 (22.2–108) ± 6.5	112 (70.1–203) ± 11 ^{*,#}	<0.001*
Waist-hip ratio	0.87 (0.790–0.960) ± 0.02	0.860 (0.790–0.980) ± 0.020	0.950 (0.810–1.09) ± 0.020 ^{*,#}	0.005*
50 kHz body phase angle	5.93 (4.70–6.60) ± 0.20	5.82 (5.10–6.70) ± 0.14	4.93 (3.60–6.70) ± 0.21 ^{*,#}	<0.001*
Physical Performance				
Grip Strength (kg/cm)	33.5 (13.3–53.4) ± 3.5	33.7 (20.5–49.6) ± 2.7	25.3 (10.5–53.4) ± 2.7	0.081
Chair Test (s)	8.14 (6.70–10.1) ± 0.30	7.93 (5.30–14.0) ± 0.63	11.9 (7.72–20.7) ± 0.5 ^{*,#}	<0.001*
Walking speed (normal) (s)	3.43 (2.76–4.43) ± 0.13	3.35 (2.23–4.02) ± 0.13	3.66 (2.60–4.08) ± 0.11	0.193
Walking speed (fast) (s)	2.12 (1.75–2.47) ± 0.07	1.99 (0.72–2.42) ± 0.12	2.54 (1.98–3.28) ± 0.11 ^{*,#}	0.002*
Inflammatory markers				
GDF-15	365 (131–1011) ± 70	350 (219–501) ± 21	626 (348–1336) ± 78 ^{*,#}	0.004*
Exosomes characterization				
Extracellular vesicles number (particles/mL)	2.10 × 10 ⁸ (2.21 × 10 ⁷ –8.27 × 10 ⁸) ± 7.91 × 10 ⁷	3.32 × 10 ⁸ (1.34 × 10 ⁷ –1.45 × 10 ⁹) ± 1.07 × 10 ⁸	9.01 × 10 ⁸ (3.09 × 10 ⁷ –5.95 × 10 ⁹) ± 4.64 × 10 ⁸	0.224
Extracellular vesicles size (nm)	140 (115–162) ± 4	142 (110–162) ± 4	139 (112–175) ± 5	0.687

Data are mean ± (SEM), range () or %.

*Statistically significant (p < 0.05). † indicates a statistically significant difference compared with the Young group (p 0.05); # indicates a statistically significant difference compared with the Middle-aged group (p 0.05).

631 known and 131 novel miRNAs, based on alignment to the human genome (GRCh38) and miRBase reference sequences. Across all age groups, the majority of reads corresponded to the “other” category—mapped sequences without known annotation—followed by reads assigned to miRNA, tRNA, and rRNA categories (Supplementary Fig. 3). A detailed breakdown of RNA biotypes (Fig. 2A) revealed that while known miRNAs were among the most abundant annotated small RNAs, a substantial portion of the EV RNA cargo mapped to repeats, exonic/intronic regions, and uncharacterized elements, highlighting the complexity and heterogeneity of EV-derived small RNAs. Interestingly, intron+ sequences were more abundant in the young group compared to middle-aged and older individuals, suggesting a potential age-related loss of regulatory RNA species derived from intronic regions. The global analysis of miRNA expression revealed distinct age-associated clustering patterns. As shown in the heatmap (Fig. 2B), several miRNAs were differentially expressed in the young group compared to both middle-aged and older individuals, supporting an early divergence in the EV miRNA signature during aging.

Differential expression analysis confirmed this trend. Volcano plots indicated a higher number of significantly dysregulated miRNAs when comparing the young group with either the middle-aged (17 upregulated, 39 downregulated; Tables 3 and 4) or the elderly group (26 upregulated, 31 downregulated) (Fig. 2C, E). In contrast, the comparison between old and middle-aged participants revealed only 23 differentially expressed miRNAs (Fig. 2D), further reinforcing the notion that the most marked transcriptomic changes in EV miRNA profiles occur early in the aging process. These age-associated shifts were further illustrated by analyzing the relative read distribution of the top-expressed miRNAs across old and young age groups (Supplementary Fig. 4). While several miRNAs showed balanced expression across young and old individuals, others—such as miR-1-3p,

miR-199b-5p, miR-200b-3p, miR-200a-3p, miR-200c-3p, miR-206, miR-378c, and miR-6529-5p, were predominantly expressed in older individuals, with read counts exceeding 80–90% in this group. This skewed age-related expression pattern supports their relevance as potential biomarkers of biological aging.

To further investigate the coordinated expression and potential biological roles of EV-associated small RNAs, we performed k-means clustering across all 39 participants based on log₂-transformed expression ratios. This analysis revealed four distinct subclusters of sRNAs, each characterized by specific expression dynamics (Supplementary Fig. 5, panel A). Subcluster 1 consisted of sRNAs with increasing expression trends, while subcluster 2 included those with stable, baseline-like expression. In contrast, subclusters 3 and 4 displayed pronounced downregulation across samples, suggestive of age-related repression. GO enrichment analysis of validated target genes for each subcluster (Supplementary Fig. 5, panel B) uncovered subcluster-specific biological signatures, including pathways involved in nuclear transport, synaptic function, and cell cycle regulation, indicating that coordinated shifts in EV miRNAs may regulate distinct cellular processes during aging.

Among the downregulated miRNAs in older individuals (Table 4), several with known links to aging and inflammation were identified, including miR-143-3p, miR-196a-5p, miR-222-3p, miR-320b, miR-335-3p, miR-543, and miR-98-5p. Notably, miR-222-3p and miR-654-5p showed highly significant downregulation (adjusted p < 0.01), suggesting strong age-associated regulatory shifts. In parallel, novel miRNAs such as novel_109 and novel_433 were also significantly downregulated in older individuals, pointing toward previously undescribed regulatory elements potentially involved in the aging process. Figure 2F summarizes the overlap and divergence of miRNA expression profiles across sex and age

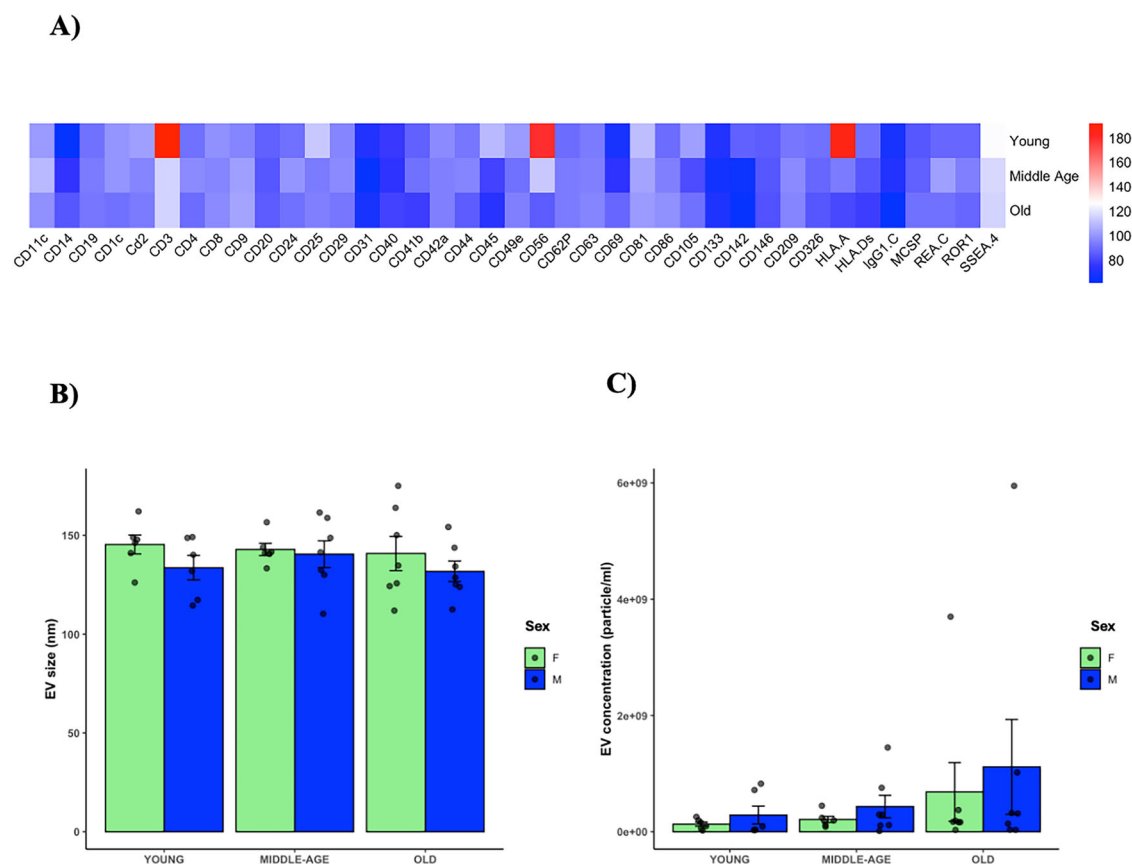


Fig. 1 | Characterization of plasma-derived EV. **A** Heatmap of EV surface epitope detection for each pool of samples grouped by age range (young, $n = 12$; middle-aged, $n = 13$; old, $n = 14$). Data are presented as the average median fluorescence intensity in the APC-H channel for each group of samples, normalized by the mean

intensity of CD9, CD63 and CD81. The percentage of expression is reflected as a color scale. Individual sample values are provided in Supplementary Table S1. Analysis of **B** particle concentration and **C** particle size by NTA for each individual sample ($n = 39$). Data is presented as mean \pm SEM according to sex and age range.

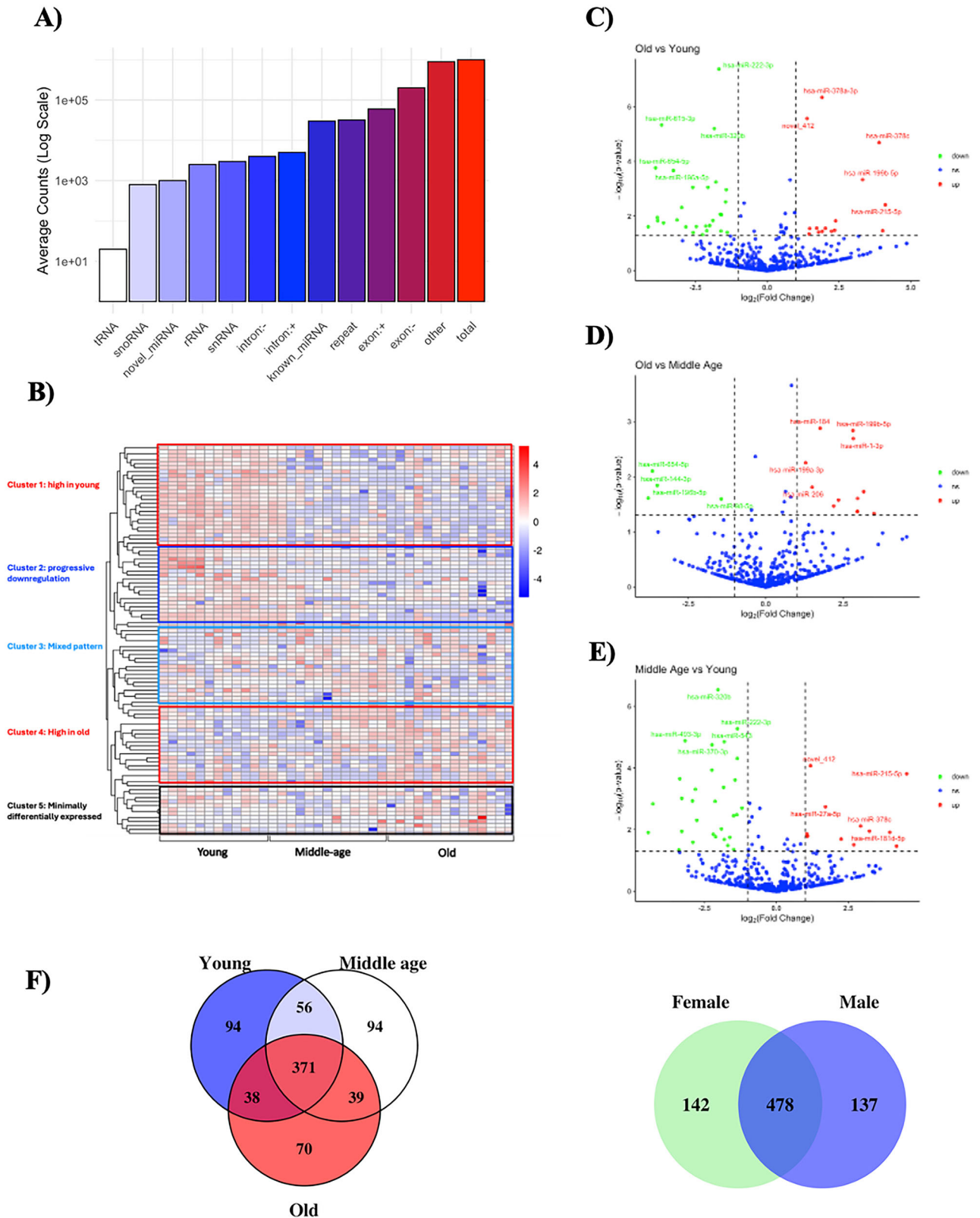
groups, revealing both shared and distinct miRNA signatures that may contribute to the molecular heterogeneity of aging. Notably, some miRNAs appeared as unique to middle-aged individuals in the Venn diagram, without overlap with either the young or old groups. This observation does not necessarily indicate statistical or biological significance but suggests that certain miRNAs were differentially expressed only in one of the middle-aged comparisons. These may represent transient or adaptive regulatory signatures characteristic of the transition from young adulthood to established aging. Although no pathway analysis was performed specifically on this subset, their intermediate pattern may reflect compensatory responses activated during midlife.

Functional enrichment of age-associated miRNA targets

To explore the potential biological significance of the age-related miRNA changes, Gene Ontology (GO) and KEGG pathway enrichment analyses were performed on the computationally predicted targets of differentially expressed miRNAs. GO analysis for the old vs. young comparison revealed significant enrichment in terms related to biological processes (BP), cellular components (CC), and molecular functions (MF) (Fig. 3A). (Additional enrichment analyses for the middle-aged vs. young and old vs. middle-aged comparisons are provided in Supplementary Fig. S6, illustrating distinct age-related biological pathways across comparisons). Among BP, the top-enriched terms included protein phosphorylation, intracellular signal transduction, DNA repair, and other processes involved in cell signaling and genome maintenance. In CC category, significant enrichment was observed in genes associated with the cytoskeleton, Golgi apparatus, and the endomembrane system, suggesting potential associations in vesicle formation, trafficking, or cellular architecture changes that occur with aging. Regarding MF, the most enriched terms included kinase

activity, nucleoside triphosphatase regulator activity, and transcription regulator activity, highlighting putative regulatory associations in signaling cascades and gene expression. Figure 3B displays a KEGG pathway enrichment analysis comparing predicted target gene expression between older and younger individuals, highlighting pathways associated with upregulated (left panel) and downregulated (right panel) miRNAs in the older group. It is important to note that miRNAs generally function as negative regulators of gene expression. Consequently, pathways enriched for targets of miRNAs upregulated in older individuals would be predicted to undergo relative suppression, whereas pathways targeted by downregulated miRNAs may experience de-repression or activation. For example, the enrichment of targets of upregulated miRNAs in the VEGF signaling pathway suggests that this pathway may face increased inhibitory pressure with aging, potentially contributing to vascular dysfunction. Conversely, pathways such as MAPK signaling, targeted by downregulated miRNAs, may become less inhibited. These regulatory relationships remain predictive and require experimental validation to confirm actual pathway activity changes.

Among pathways linked to upregulated miRNAs, notable enrichments include the Ras signaling pathway, Th1 and Th2 cell differentiation, glycerophospholipid metabolism, leukocyte transendothelial migration, glutamatergic synapse, VEGF signaling, regulation of actin cytoskeleton and oxytocin signaling pathways. These pathways are involved in immune response modulation, vascular and synaptic signaling, and hormonal regulation. For pathways associated with downregulated miRNAs, older individuals show significant reductions in pathways such as non-small cell lung cancer, neuroactive ligand-receptor interaction, dopaminergic synapse, circadian entrainment, and MAPK signaling. Other pathways linked to downregulated miRNAs



include Axon guidance, Th17 cell differentiation, adrenergic signaling in cardiomyocytes, and Cell adhesion molecules, many of which are crucial for neural function, hormone response, and cellular communication. Together, these results suggest substantial age-associated changes in immune, endocrine, neuronal, and metabolic signaling pathways, which may reflect both adaptive and maladaptive responses to aging. However,

these computational predictions require experimental validation to confirm functional relevance.

Association between EV characteristics and clinical variables

We next examined the relationship between EV concentration and size with clinical and functional aging markers. Correlation heatmaps revealed that

Fig. 2 | sRNA profile of plasma-derived EV. **A** Classification of EV-associated small RNAs by biotype. Bar chart showing the average read counts (log scale) of different small RNA biotypes identified in plasma-derived EVs. Annotation followed a hierarchical structure: known miRNA > novel miRNA > rRNA > tRNA > snRNA > snoRNA > repeat > exon > intron > other. While miRNAs were among the most abundant annotated classes, a considerable fraction of reads mapped to non-coding elements such as repeats, intronic/exonic regions, and an unclassified “other” category. **B** Cluster analysis of the differences between miRNA expressions. Colored boxes on the left indicate distinct microRNA clusters with differential expression patterns across age groups. The overall result of the (transcript per million) TPM cluster analysis is grouped by the $\log_{10}(\text{TPM} + 1)$ value. The color

scale from red to blue represents the level of miRNA expression. **C, D, E** Volcano diagrams comparing the miRNA expression between the old versus the young group (**C**), the old versus the middle-age groups (**D**) and the middle-age versus the young groups (**E**). The *x*-axis shows the fold-change (FC) in miRNA expression between different samples, and the *y*-axis shows the statistical significance of the differences between groups. Differentially expressed miRNAs are considered to be those with $\log_2\text{FC} > 1$ and *p*-value < 0.05. **F** Venn diagrams illustrating the overlap and uniqueness of significantly dysregulated miRNAs (FDR < 0.05) across pairwise age group comparisons (young vs. middle-aged; young vs. old; middle-aged vs. old), stratified by sex. Numbers indicate the count of unique and shared differentially expressed miRNAs.

Table 3 | Old vs. young up-regulated miRNA expression profile

	sRNA	Log ₂ FC	p-value	Adjusted p-value
Up-regulated	hsa-miR-125b-1-3p	-2.14	0.02	0.17
	hsa-miR-1301-3p	-3.61	0.02	0.15
	hsa-miR-1307-3p	-0.92	0.01	0.11
	hsa-miR-134-5p	-2.00	0.02	0.17
	hsa-miR-143-3p	-1.43	0.001	0.02
	hsa-miR-149-5p	-2.98	0.005	0.07
	hsa-miR-196a-5p	-3.27	2.17E-04	0.01
	hsa-miR-196b-5p	-2.47	0.02	0.17
	hsa-miR-22-5p	-3.14	0.01	0.13
	hsa-miR-222-3p	-1.69	4.17E-08	1.05E-05
	hsa-miR-224-5p	-1.64	0.01	0.10
	hsa-miR-26a-5p	-0.45	0.04	0.19
	hsa-miR-320a-3p	-0.81	0.003	0.05
	hsa-miR-320b	-1.84	6.31E-06	3.18E-04
	hsa-miR-320c	-1.60	0.01	0.10
	hsa-miR-335-3p	-2.60	0.001	0.02
	hsa-miR-365a-5p	-2.58	0.04	0.19
	hsa-miR-365b-5p	-2.84	0.03	0.17
	hsa-miR-409-3p	-1.45	0.003	0.05
	hsa-miR-4488	-2.26	0.05	0.21
	hsa-miR-450a-5p	-3.83	0.01	0.11
	hsa-miR-485-5p	-1.61	0.04	0.19
	hsa-miR-493-3p	-1.89	0.01	0.13
	hsa-miR-493-5p	-1.39	0.04	0.19
	hsa-miR-543	-2.07	0.001	0.02
	hsa-miR-615-3p	-3.68	4.65E-06	2.93E-04
	hsa-miR-654-5p	-3.89	1.73E-04	0.01
	hsa-miR-671-3p	-2.10	0.03	0.19
	hsa-miR-98-5p	-1.79	0.001	0.01
	novel_109	-4.15	0.02	0.17
	novel_433	-3.82	0.01	0.13

Table 4 | Old vs. young down-regulated miRNA expression profile

	sRNA	Log ₂ FC	p-value	Adjusted p-value
Down-regulated	hsa-miR-125b-1-3p	-2.14	0.02	0.17
	hsa-miR-1301-3p	-3.61	0.02	0.15
	hsa-miR-1307-3p	-0.92	0.01	0.11
	hsa-miR-134-5p	-2.00	0.02	0.17
	hsa-miR-143-3p	-1.43	0.001	0.02
	hsa-miR-149-5p	-2.98	0.005	0.07
	hsa-miR-196a-5p	-3.27	2.17E-04	0.01
	hsa-miR-196b-5p	-2.47	0.02	0.17
	hsa-miR-22-5p	-3.14	0.01	0.13
	hsa-miR-222-3p	-1.69	4.17E-08	1.05E-05
	hsa-miR-224-5p	-1.64	0.01	0.10
	hsa-miR-26a-5p	-0.45	0.04	0.19
	hsa-miR-320a-3p	-0.81	0.003	0.05
	hsa-miR-320b	-1.84	6.31E-06	3.18E-04
	hsa-miR-320c	-1.60	0.01	0.10
	hsa-miR-335-3p	-2.60	0.001	0.02
	hsa-miR-365a-5p	-2.58	0.04	0.19
	hsa-miR-365b-5p	-2.84	0.03	0.17
	hsa-miR-409-3p	-1.45	0.003	0.05
	hsa-miR-4488	-2.26	0.05	0.21
	hsa-miR-450a-5p	-3.83	0.01	0.11
	hsa-miR-485-5p	-1.61	0.04	0.19
	hsa-miR-493-3p	-1.89	0.01	0.13
	hsa-miR-493-5p	-1.39	0.04	0.19
	hsa-miR-543	-2.07	0.001	0.02
	hsa-miR-615-3p	-3.68	4.65E-06	2.93E-04
	hsa-miR-654-5p	-3.89	1.73E-04	0.01
	hsa-miR-671-3p	-2.10	0.03	0.19
	hsa-miR-98-5p	-1.79	0.001	0.01
	novel_109	-4.15	0.02	0.17
	novel_433	-3.82	0.01	0.13

vesicle concentration was significantly associated with multiple aging-related clinical variables in an age-dependent manner (Fig. 4A). Vesicle size showed weaker and more variable associations (Fig. 4B). Specifically, vesicle concentration was negatively correlated with markers of adiposity and positively correlated with physical function metrics, particularly in younger individuals. Correlations between log-transformed plasma EV concentration and key clinical variables were assessed in the overall cohort (top panels) and stratified by sex (bottom panels) (Fig. 5A, B). Significant

negative correlations were observed between EV concentration and muscle quality ($r = -0.422, p = 0.007$), and positive correlations with waist-to-hip ratio ($r = 0.365, p = 0.022$). Stratified analyses revealed that the inverse association between EV concentration and muscle quality was particularly strong in males ($r = -0.698, p < 0.001$). EV concentration was also positively associated with visceral fat in males ($r = 0.490, p = 0.028$). Regarding physical function associations, EV concentration was positively correlated with walking speed and the chair test ($r = 0.318, p = 0.048$ and $r = 0.365,$

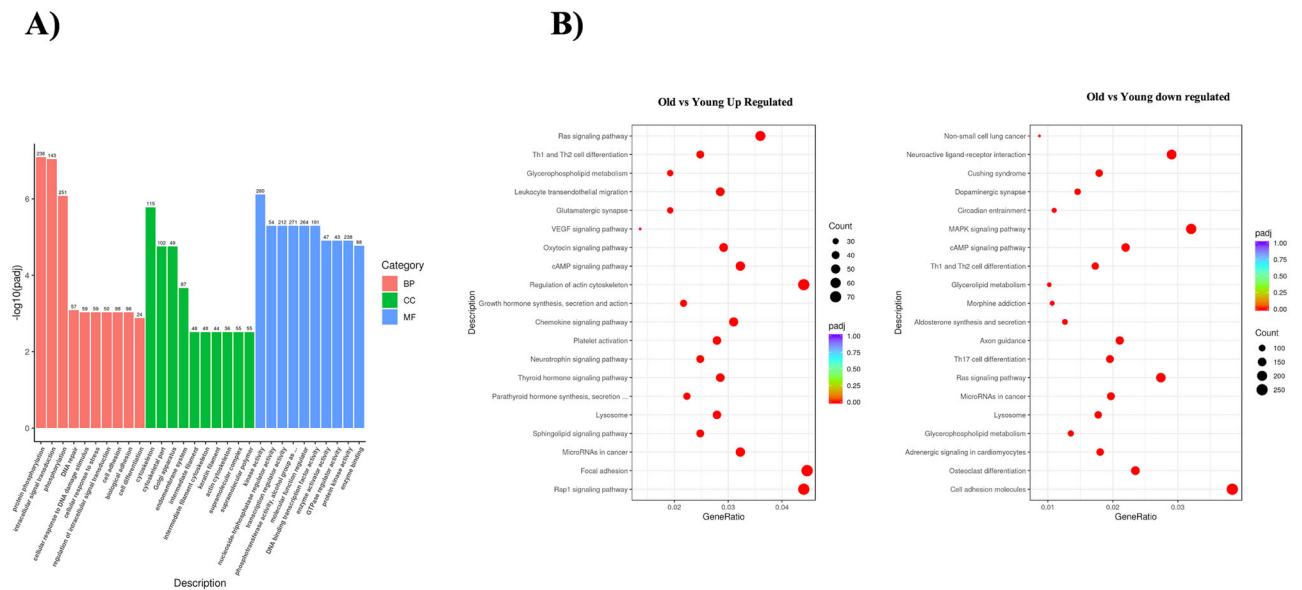


Fig. 3 | Old vs. young GO and KEGG enrichment analysis of different expressed miRNA targets. **A** Histogram showing GO enrichment analysis and GO terms for biological process (red), cellular component (green), and molecular function (blue) categories. The x-axis represents the GO terms, and the y-axis represents the number of genes. **B** KEGG enrichment analysis of co-differentially expressed pathways in old vs. young participants. The horizontal axis represents the gene ratio (number of

target gene candidates related to a specific term), old vs. Young, the circle size indicates the number of all genes in the GO category, and the scale color depicts the corrected *p*-value. GO terms with *p*-adj < 0.05 are considered significantly enriched. The size of the dots indicates the number of genes involved in each pathway, while the color represents statistical significance (adjusted *p*-value), with red indicating the highest significance.

p = 0.022), but not significantly associated with grip strength in the overall sample. When stratified by sex, EV concentration showed a positive association with fast walking speed in both females (*r* = 0.465, *p* = 0.031) and males (*r* = 0.467, *p* = 0.039), and a trend toward significance in the chair test in males (*r* = 0.273, *p* = 0.144). These associations suggest that EV concentration may reflect early changes in functional capacity and metabolic health.

EV-associated miRNAs correlate with functional and biological aging proxies

To further explore the potential relevance of EV-derived miRNAs as candidate markers of biological and functional aging, we performed regression analyses between individual miRNAs and key clinical proxies of health status. In this study, biological aging was operationalized through GDF-15 levels and functional capacity measures (grip strength, gait speed, chair stand performance), which together capture the multi-dimensional nature of the aging process beyond chronological age alone. As expected, GDF-15 levels were positively correlated with chronological age (data not shown), supporting its validity as a biological aging marker in our cohort. (Supplementary Fig. 7). However, the moderate correlation coefficient indicates that GDF-15 captures variance in aging-related physiology beyond chronological time alone, consistent with its role as a marker of biological rather than solely chronological aging. We assessed associations between miRNA expression levels and waist-to-hip ratio, muscle quality, visceral fat area, adherence to the Mediterranean diet (Predimed score), and GDF-15 levels, as well as physical performance metrics such as the chair stand test, grip strength and gait speed (normal and fast). Linear regression analyses included all detected miRNAs with mean expression >10 TPM across samples (*n* = 156 miRNAs) to ensure adequate detection levels. Each clinical outcome was modeled separately as: Outcome ~Age + Sex + miRNA expression (see methods section). The results are summarized in volcano plots (Fig. 6), which display the beta coefficients and statistical significance for each miRNA-phenotype association. For the waist-to-hip ratio, miRNAs such as let-7d-5p, miR-30e-3p, and miR-340-5p showed the strongest associations, predominantly negative. In the case of the Predimed score, higher levels of miR-361-3p, miR-340-5p, and miR-451a were associated

with healthier dietary patterns. Regarding muscle quality, miR-125b-5p, miR-140-3p, miR-320b, and miR-122-5p showed negative associations, suggesting a potential correlation with reduced muscle performance. For GDF15, a well-established marker of biological aging^{26,27}, miR-320b, miR-30a-5p, miR-381-3p, and miR-320c emerged as the most strongly associated miRNAs. Lastly, let-7d-5p, miR-30c-5p, and miR-30a-5p were among the top miRNAs associated with visceral fat. In the chair stand test, miRNAs such as miR-320a-3p, miR-320b, miR-125b-5p, miR-361-3p, and miR-320c showed positive associations with better performance, while miR-27a-5p showed a negative association. For fast walking speed, miR-142-5p, let-7i-5p, miR-181a-5p, and miR-101-3p emerged as top candidates with positive associations, whereas miR-200b-3p showed a negative association. For normal walking speed, just 3 miRNAs were significant: miR-425-5p, miR-320a-3p, and miR-421-3p. Finally, in the grip strength model, miR-140-3p and miR-320b were among the miRNAs most strongly associated. Altogether, these correlative findings highlight specific EV-carried miRNAs as candidates for biomarkers of age-related physiological alterations and health trajectories.

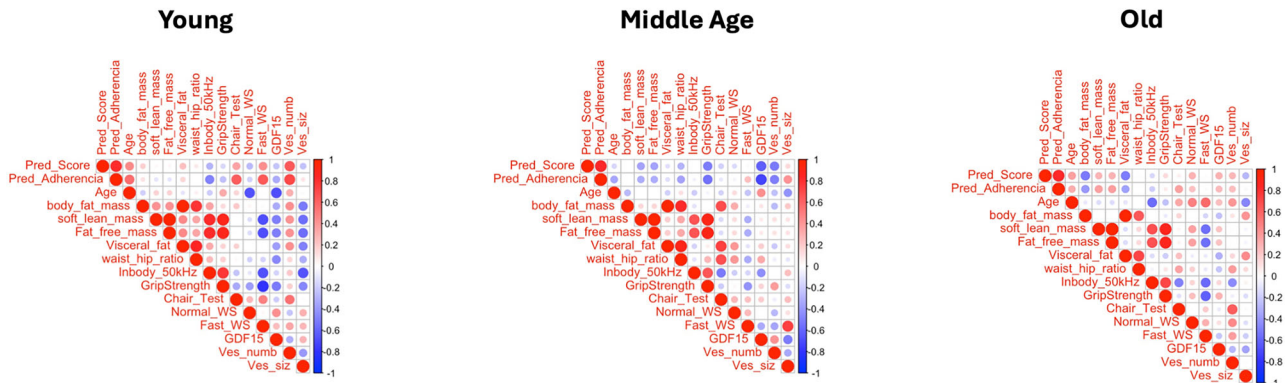
Discussion

In this study, we characterized plasma-derived EVs across healthy aging and identified age-associated miRNA signatures predominantly reflecting musculoskeletal and metabolic changes, with secondary alterations in immune and neurological pathways.

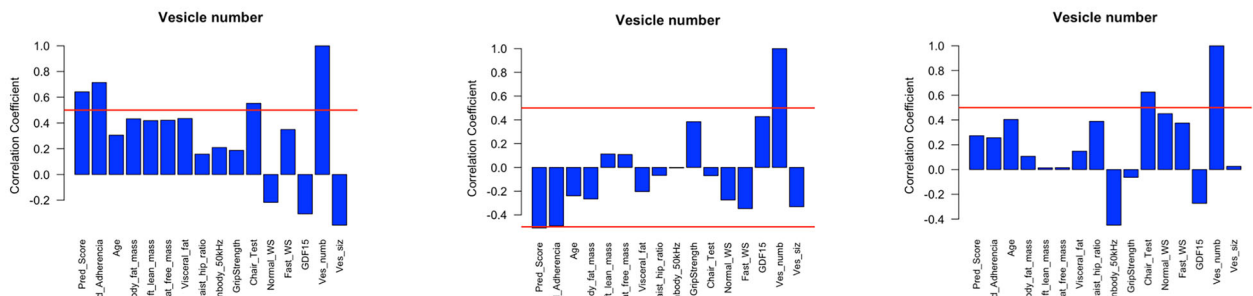
Our findings align with previous research indicating that EVs play a crucial role in intercellular communication and are involved in various physiological and pathological processes, including aging and age-related diseases^{11,28}. Interestingly, contrary to previous reports suggesting a decline in EV concentration with age²⁸, we observed a trend toward increased EV concentration in older individuals. This discrepancy may reflect age-related changes in vesicle biogenesis, release, or clearance mechanisms, warranting further investigation¹⁹. In fact, a recent report has proposed that alterations in the release of EV could be considered an emerging hallmark of aging, as EV secretion patterns are associated with cellular and senescence status⁹.

On the other hand, the age-dependent variation in EV surface markers—including decreased CD3, CD56, HLA-A, and CD45 and increased CD14

A)



B)



C)

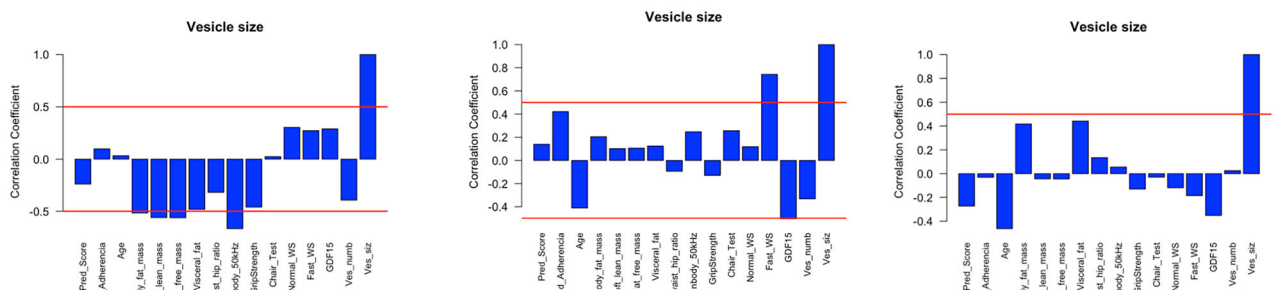


Fig. 4 | Association between vesicle number and vesicle size with all the clinical variable included in the study by age groups. Heatmaps show the correlation among all the variables by age group (A) and the bar plots the specific correlation

coefficient between vesicle number (B) and size and all the variables by age groups (C). The red line shows the correlation coefficients that are significant.

and CD69—supports a shift in EV immunophenotype, consistent with immunosenescence and changes in circulating immune cell populations²⁹. These changes could reflect a reduced contribution of adaptive immune cells to the pool of circulating EVs and an increased release by activated monocytes³⁰. Interestingly, recent findings have shown that EV surface antigen profiling can be used as a biomarker of aging, reflecting features of inflammaging commonly observed in older people, as well as the

cardiovascular risk of individuals³¹. Furthermore, the alterations in the surface markers of EVs could not only indicate a differential cellular origin but could also affect the uptake of these EVs by different target cells³². This could ultimately influence the intercellular communication mediated by EVs during aging.

The analysis of EV-associated small RNAs revealed distinct clustering by age group, with the young cohort showing a markedly different profile

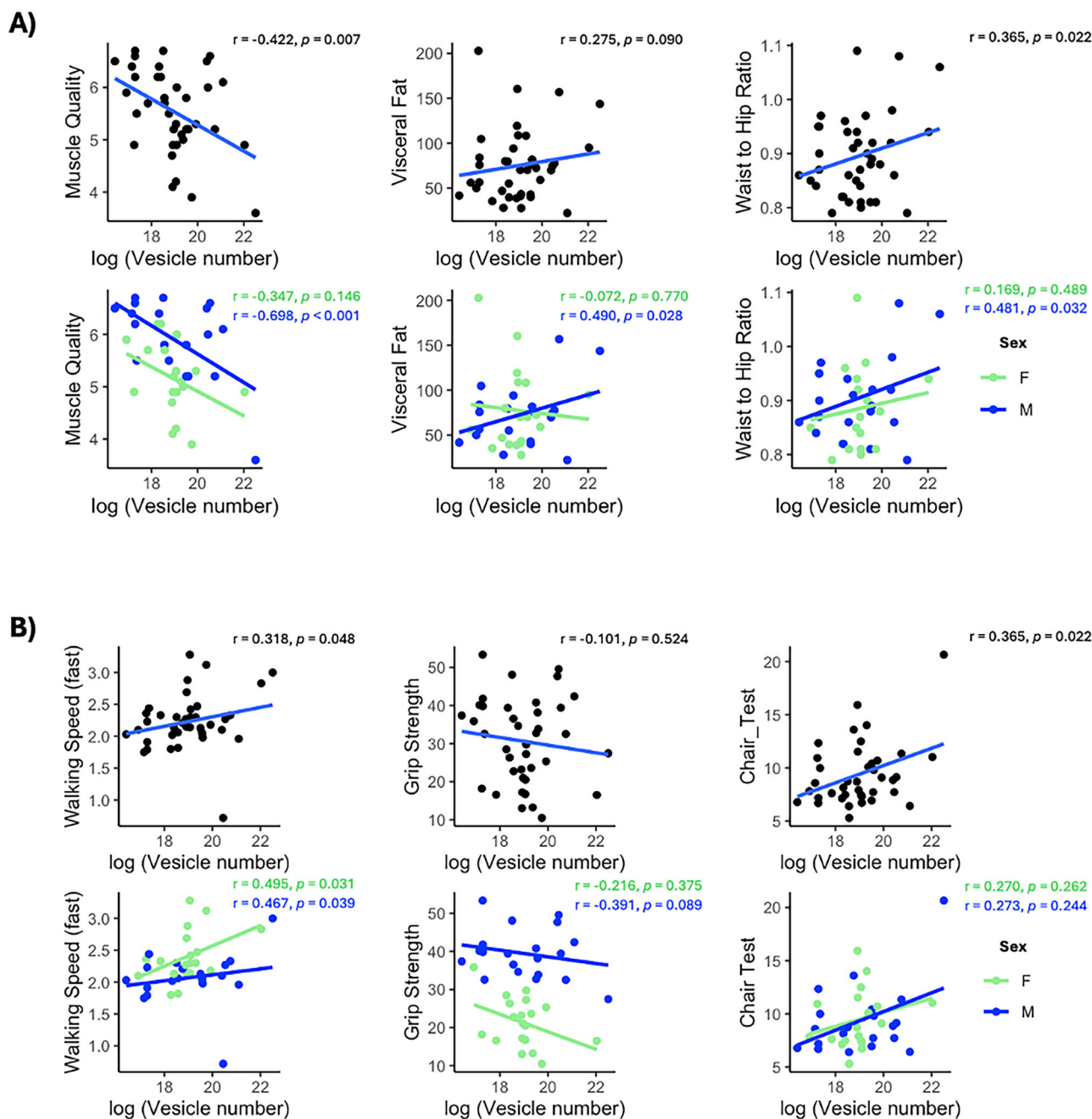


Fig. 5 | Associations between EV concentration and clinical/functional aging markers, stratified by sex. A Scatterplots show associations between log-transformed EV concentration and three aging-related physiological variables: muscle quality, visceral fat content, and waist-to-hip ratio. Top panels represent all individuals; bottom panels show stratified analyses by sex (green = females, blue =

males). EV concentration was negatively associated with muscle quality and positively associated with adiposity markers, particularly in males. B Associations between log-transformed EV concentration and physical function indicators: fast walking speed, grip strength, and chair stand test performance. Similar to panel A, top panels show the full cohort, and bottom panels show sex-stratified analyses.

compared to middle-aged and older individuals. This early divergence in the EV miRNA signature suggests that some molecular hallmarks of aging are already encoded in EVs well before late-life decline becomes clinically evident. Among the downregulated miRNAs in older individuals, several have known roles in aging-related pathways, including miR-143-3p, miR-196a-5p, miR-222-3p, and miR-320b^{33–35}. Notably, miR-222-3p—implicated in vascular aging and endothelial dysfunction—was significantly reduced in older individuals, in line with its reported decline in age-related vascular disease contexts^{34,36–39}.

One of the most important findings of our study was the predominant expression of several miRNAs in EVs from older individuals, including miR-206, a well-characterized muscle-specific miRNA (“myomiR”). miR-

206 plays a pivotal role in skeletal muscle regeneration, satellite cell differentiation, and neuromuscular junction remodeling^{37–41}. It is known to be upregulated in response to muscle injury and sarcopenia, suggesting a compensatory mechanism in aging muscle. While previous studies have not definitively shown miR-206 enrichment in EVs from older adults, our findings provide the first evidence that miR-206 may be exported in EVs during aging, positioning it as a minimally invasive biomarker of muscle degeneration and functional capacity.

In addition to miR-206, several other miRNAs—miR-122-5p, miR-143-3p, miR-99b-5p, and miR-20b-3p—also showed strong age-associated enrichment in EVs. These miRNAs are linked to key biological processes relevant to aging, such as lipid metabolism (miR-122-5p), insulin resistance

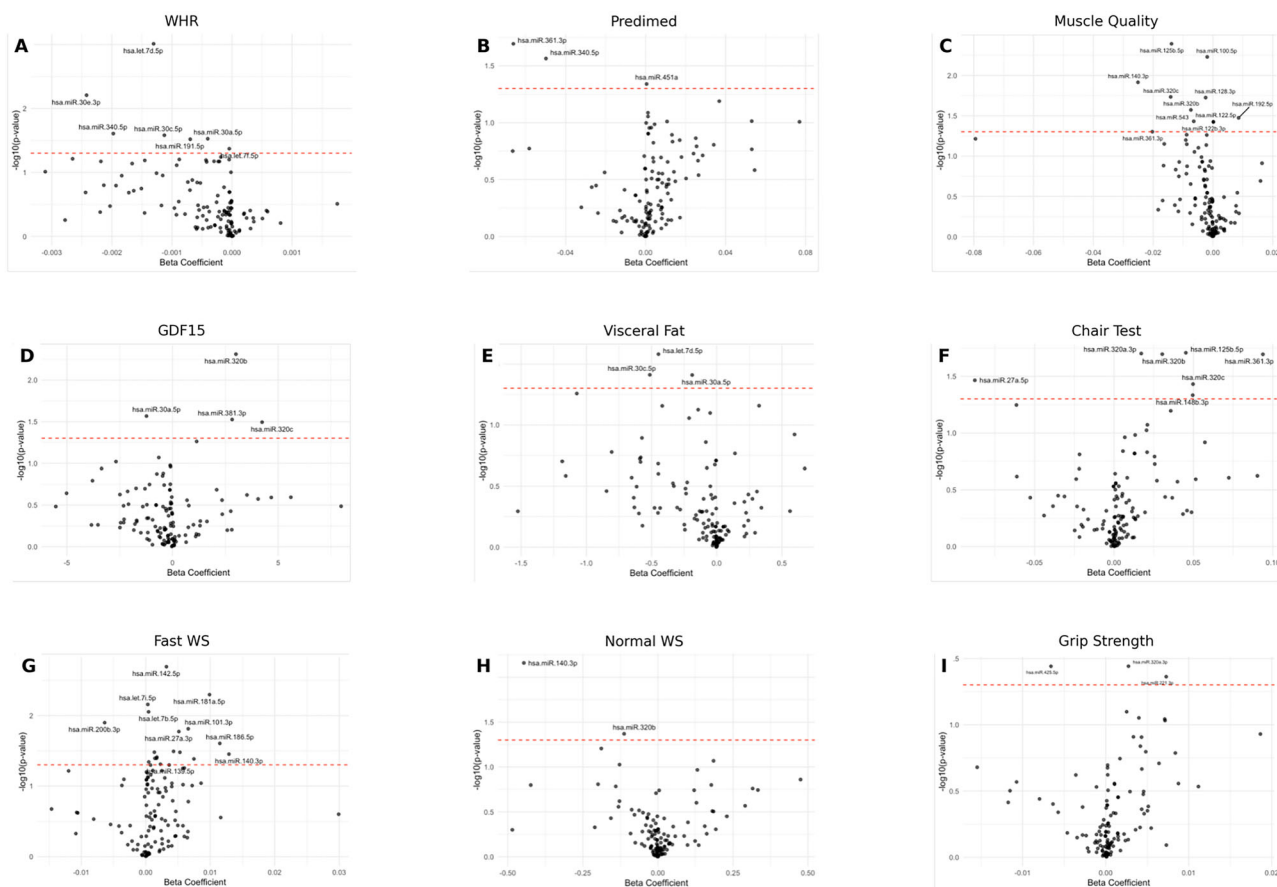


Fig. 6 | Associations between EV-derived miRNAs and proxies of aging-related health status. Volcano plots show the results of linear regression analyses evaluating associations between individual plasma EV-derived miRNAs and selected clinical proxies of aging. The x-axis represents the beta coefficient for each miRNA, and the y-axis shows the $-\log_{10}(p\text{-value})$ of the association. Labeled miRNAs represent those with the strongest associations within each phenotype. These analyses were adjusted for chronological age and sex. Several miRNAs, including miR-30e-3p, miR-222-3p,

and miR-320c, showed consistent associations across multiple phenotypes, supporting their potential as biomarkers of functional and biological aging. The Beta coefficients were extracted from the regression of the outcome \sim Age + miRNAs. **A** waist-to-hip ratio; **B** Predimed score, **C** muscle quality (50 kHz phase angle, InBody); **D** plasma GDF-15; **E** visceral fat (InBody); **F** chair test; **G** fast WS (walking speed); **H** normal WS (walking speed); **I** grip strength.

and muscle aging (miR-143-3p), and vascular remodeling (miR-20b-3p)^{42–44}. The combined presence of these miRNAs in EVs suggests an integrated molecular response to systemic stress, particularly in metabolically active tissues like skeletal muscle, which undergo significant remodeling with age. Interestingly, miR-6529-5p was one of the most highly expressed miRNAs in older individuals in our relatively healthy aging cohort. This finding differs from recent evidence reporting significant downregulation of miR-6529-5p in plasma exosomes of patients with Alzheimer’s disease, where lower levels were associated with worse cognitive performance⁴⁵. Rather than a direct contradiction, this difference may reflect distinct biological contexts—healthy aging versus neurodegenerative disease. In our cohort, the upregulation of miR-6529-5p could indicate a compensatory or protective mechanism aimed at preserving cognitive or cellular function during healthy aging. This hypothesis requires functional validation but suggests that miR-6529-5p trajectories may differ between resilient and pathological aging and could potentially serve as a biomarker distinguishing these trajectories.

The KEGG pathway enrichment analysis highlights significant transcriptional alterations associated with aging, reflecting both adaptive and maladaptive changes across various biological systems. Notably, the upregulation of the Ras signaling pathway in older individuals suggests enhanced cellular proliferation and survival mechanisms, which have been linked to longevity assurance and metabolic regulation⁴⁶. Similarly, the increased activity in VEGF signaling pathways may represent a compensatory response to age-related vascular insufficiencies, as augmenting VEGF

signaling has been shown to prevent capillary loss and improve organ function in aged models⁴⁷. The enrichment of Th1 and Th2 cell differentiation pathways indicates a shift in immune response dynamics with age, potentially contributing to altered inflammatory profiles observed in the elderly⁴⁸. In the nervous system, upregulated glutamatergic synapse pathways may reflect attempts to maintain excitatory neurotransmission amidst age-related synaptic decline. Additionally, changes in oxytocin signaling pathways could influence social and emotional behaviors in aging populations, given oxytocin’s role in socioemotional processing^{49,50}. Conversely, the downregulation of pathways such as dopaminergic synapse and circadian entrainment underscores potential vulnerabilities in neurochemical signaling and circadian regulation with age. Reduced dopaminergic activity has been associated with cognitive decline in aging, while alterations in circadian rhythms can impact sleep quality and overall health^{51,52}. The observed decrease in MAPK signaling pathways further suggests diminished cellular stress responses and regenerative capacities in older individuals. Collectively, these findings provide an initial characterization of the molecular shifts occurring with aging, highlighting potential targets for interventions aimed at mitigating age-associated functional declines. Importantly, we also observed strong associations between EV concentration and miRNA content with clinical and functional indicators of aging, such as visceral fat, muscle quality, grip strength, gait speed, and chair stand performance. These associations remained significant even after adjusting for chronological age, supporting the utility of EV-associated miRNAs as proxy markers of biological rather than chronological aging. Consistently, a recent

study demonstrated that plasma EV content is linked to frailty status in older adults, further suggesting that these particles could serve as indicators of functional capacity⁵³. In this sense, EVs have been proposed as central players involved in the hallmarks of aging, contributing to age-promoting processes such as DNA damage, inflammatory signaling spread, or impairment of stem cell function. However, EVs have also demonstrated the potential to reduce the age-related decline in physical performance by promoting autophagy, mitochondrial function, or telomere repair⁵⁴.

Despite the strengths of this study—including multimodal EV profiling and integration with functional clinical metrics—several limitations should be acknowledged. First, the observational and cross-sectional nature of the study precludes any conclusions regarding causality. While we identified associations between EV features and biological aging markers, it remains unclear whether changes in EV composition actively contribute to aging phenotypes or merely reflect downstream consequences. Longitudinal studies tracking EV dynamics over time, ideally alongside changes in muscle and metabolic function, are needed to disentangle cause-and-effect relationships. Second, our sample size, while sufficient to detect significant differences, was relatively modest and composed of a predominantly healthy aging population. The limited sample size precluded comprehensive adjustment for potential confounders such as medication use, specific comorbidities, physical activity levels, and smoking history in multivariable models. While our study included generally healthy individuals, residual confounding cannot be excluded. Future studies with larger cohorts are needed to validate these associations with appropriate confounder adjustment and to determine whether the observed EV-miRNA signatures are independent of other age-related factors. These results should therefore be considered exploratory and hypothesis-generating rather than definitive. Third, while our EV isolation and characterization methods followed MISEV2023 guidelines and included size exclusion chromatography using qEVoriginal/70 nm columns (which effectively separates EVs from the majority of free-circulating RNA-protein complexes, soluble proteins, and lipoprotein particles based on size), we did not perform RNase protection assays to definitively confirm that detected miRNAs represent internal EV cargo rather than surface-associated RNAs. However, several lines of evidence support that our detected miRNAs predominantly represent bona fide EV cargo: (1) size exclusion chromatography is recognized in MISEV2023 guidelines as a method that significantly reduces copurification of non-vesicular extracellular RNA; (2) our multi-step isolation protocol combining SEC with subsequent RNA extraction using validated kits minimizes contamination from free ribonucleoprotein complexes; (3) we detected classical EV-enriched miRNAs known to be predominant EV cargo (e.g., miR-122, miR-320 family, let-7 family); and (4) the miRNA profiles we observed are consistent with previous EV-miRNA studies using similar SEC-based isolation methods. Nevertheless, future studies employing RNase protection assays (e.g., ref. 54) combined with qPCR validation would provide additional direct confirmation of cargo localization for specific miRNA candidates. Fourth, although we report strong correlations between EV-associated miRNAs and functional measures such as gait speed and muscle quality, the biological activity of these miRNAs in recipient cells remains speculative. Functional validation using cell-based assays and in vivo models is needed to determine whether these EV miRNAs are taken up by target tissues (e.g., muscle, endothelium, brain) and whether they mediate specific phenotypic effects.

Finally, our analysis focused primarily on small RNAs, particularly miRNAs, within EVs. However, EVs also contain other molecular cargo—including proteins, lipids, and long non-coding RNAs—that may play critical roles in aging. Future studies employing multi-omics approaches (e.g., proteomics, lipidomics, transcriptomics) could provide a more holistic understanding of EV-mediated signaling in aging. Moving forward, interventional studies examining EV dynamics pre- and post-intervention could elucidate whether EV profiles are modifiable and whether changes reflect improvements in biological aging markers. Proof-of-concept studies have demonstrated that EV profiles can be altered by acute interventions in non-aging contexts (e.g., exercise (see ref. 55)), suggesting that similar approaches

may be valuable for understanding EV dynamics in aging populations⁵⁶. Future work should examine whether lifestyle or pharmacological interventions targeting healthy aging produce measurable changes in EV-miRNA signatures. Based on our findings, preliminary evidence suggests a model in which plasma-derived EVs serve as dynamic conveyors of aging-related molecular information, particularly from skeletal muscle and metabolic tissues. The miRNA signatures they carry may offer novel avenues for biomarker discovery, patient stratification, and the design of targeted interventions to promote healthy aging and preserve muscle function. Critically, all findings reported here are correlative in nature. We have not performed functional validation experiments to demonstrate that the identified EV-miRNAs are taken up by recipient cells, successfully suppress their predicted target genes, or causally influence the biological processes identified through pathway enrichment. Such functional validation through cell-based assays and in vivo models represents an essential next step to establish causality.

Methods

Study population

This study included 39 participants from the Balearic Islands Study of Aging (BILSA Study), a prospective open cohort initiated in January 2022 in the Mallorca Island area. Participants were recruited between February and October 2022 at the Hospital Universitari Son Espases. All individuals underwent a comprehensive 3-h assessment, including physiological, psychological, and medical evaluations conducted by trained personnel to assess general health status and physical function. Participants were generally healthy and community-dwelling adults. Individuals with well-controlled chronic conditions such as hypertension, diabetes, or hypercholesterolemia were eligible. Age categories were defined a priori based on biological life stages commonly used in aging research: young adults (20–33 years, representing post-developmental maturity), middle-aged adults (39–56 years, representing the transition period), and older adults (≥ 60 years, representing established aging). We acknowledge that these discrete categories may not optimally capture continuous age-related changes and that boundary effects may exist. Former and occasional smokers were also included. Exclusion criteria comprised cognitive impairment, neuromuscular or muscular diseases, and a history of cancer within the previous ten years. To minimize confounding due to transient inflammatory responses, participants were instructed to refrain from exercise 24 h prior to the study visit. All individuals were thoroughly informed about the study objectives, procedures, and potential risks. The study was conducted in accordance with the ethical principles of the Declaration of Helsinki and approved by the Ethics Committee of the Balearic Islands (Comitè d'Ètica de la Investigació de les Illes Balears; IB 4337/20 PI). Written informed consent was obtained from all participants prior to enrollment. Blood samples were collected from each participant and stored at -80°C in the Biobank Unit for subsequent analyses. Clinical data collected included age, sex, smoking status, comorbidities, and results from a fasting blood test.

Clinical and functional assessments

Clinical and functional characterization of participants was performed following standardized protocols as previously described by our group²⁶. Briefly, body composition parameters, including body fat mass, soft lean mass, fat-free mass, visceral fat area, waist-to-hip ratio, and 50kHz body phase angle, were assessed using multi-frequency bioelectrical impedance analysis (InBody S10, InBody Co., Seoul, South Korea). Phase angle reflects cellular membrane integrity and muscle quality, with lower values indicating reduced muscle health^{57,58}. Physical performance was evaluated through grip strength measurements using a hydraulic hand dynamometer (KERN MAP 80 K1, KERN, Germany), the five-repetition chair stand test, and gait speed assessment at both normal and fast pace over a 4-meter course. GDF-15 (growth differentiation factor-15) was selected as a marker of biological aging due to its consistent elevation with chronological age across populations and its strong associations with multiple age-related diseases, physical function decline, frailty, and all-cause mortality risk^{26,27}.

Plasma GDF-15 concentrations were quantified using a commercially available ELISA kit (R&D Systems, Minneapolis, MN, USA). Finally, adherence to the Mediterranean diet was assessed using the validated 14-item PREDIMED questionnaire.

EV isolation

EVs were isolated by qEVoriginal/70 nm Gen 2 size exclusion columns (Izon Science, Christchurch, NZ). As per the manufacturer's instructions, 500 μ L of samples were successively centrifuged, first at 1500 \times g for 10 min and subsequently at 10,000 \times g for 10 min, with a constant temperature of 4 °C in both cases. Columns were flushed with 17 mL of commercial PBS (Capricorn Scientific, Ebsdorfergrund, DE), 0.22- μ m filtered. Samples were added on top of qEV columns, and 0.4 mL fractions were collected. Four fractions of 0.4 mL corresponding to the Purified Collection Volume (PCV) were pooled, aliquoted and stored at -80 °C until further analysis.

EV characterization

Size and concentration profile of EVs were acquired for each individual sample by Nanosight NS300 (Malvern Instruments, Malvern, UK). Diluted samples were analyzed by capturing five consecutive videos with a syringe pump speed of 50. A sCMOS camera and green laser type were used, and data were processed with NTA 3.2 Dev Build 3.2.16 Software. A total of 37 EV surface markers were analyzed by flow cytometry (BD FACSVerser, BDBiosciences, United States) using the human MACSPlex EV Kit IO (Miltenyi Biotec, Bergisch Gladbach, DE), according to the manufacturer's short protocol. Sample pools were made according to age group (young, $n = 12$; middle-aged, $n = 13$; old, $n = 14$), and 1.3 μ g of protein was used for each sample pool. The average fluorescence medians of CD9, CD63, and CD81 in the APC-H channel were used to normalize the fluorescence of each sample for data analysis.

RNA isolation, sRNA profile, and bioinformatic analysis

Total RNA was isolated from EVs using the miRNeasy Serum/Plasma kit (Qiagen, Hilden, DE) following the manufacturer's instructions. Briefly, five volumes of QIAzol Lysis Reagent were added to 200 μ L of each sample, followed by the incorporation of chloroform and centrifugation for 15 min at 12,000 \times g at 4 °C. Upper phase was transferred to a new tube, mixed with absolute ethanol (Sharlab S. L, Barcelona, ES) and pipetted into an RNeasy MinElute spin column. After centrifugation at 8000 \times g for 15 s, several cleansing steps were performed with RWT and RPE buffers. Finally, 80% ethanol was added to the column, centrifuged for 2 min at 8000 \times g, and RNA was eluted in 12 μ L RNase-free water. RNA concentration was measured spectrophotometrically (NanoDrop™ 2000/2000c, Thermo Fisher Scientific). Small RNA libraries were constructed following the manufacturer's protocol. Briefly, 3' and 5' adapters were sequentially ligated to small RNAs, followed by reverse transcription to synthesize first-strand cDNA and PCR amplification. Libraries were sequenced on an Illumina platform (Novogene, Beijing, China) using single-end 50 bp reads. Expression normalization and data quality control were performed using TPM (Transcripts Per Million) values \log_{10} -transformed for downstream analyses. Density distributions were inspected to ensure uniformity across samples, and a Pearson correlation matrix was computed to assess the consistency of expression profiles between samples. Samples with $R^2 > 0.85$ were retained for analysis (see Supplementary Fig. 1).

Statistical analysis

All statistical analyses were performed using R version 4.2.3 (R Core Team, 2023) and relevant Bioconductor packages. Descriptive statistics were calculated for all demographic and clinical variables. Data are presented as mean \pm standard deviation (SD) for normally distributed variables or median with interquartile range (IQR) for non-parametric data. Normality was assessed using the Shapiro–Wilk test. For group comparisons across age (young, middle-aged, and old) or sex, we used one-way ANOVA or Kruskal–Wallis tests for continuous variables, followed by post-hoc Tukey's or Dunn's tests where appropriate.

Categorical variables were compared using chi-square tests. EV concentration and particle size were analyzed using linear models to assess differences across age and sex groups, and trends were evaluated using Spearman's rank correlation. EV surface marker expression data obtained from the MACSPlex assay were normalized and analyzed using heatmaps and hierarchical clustering. Differential surface marker expression across age groups was assessed using limma-based linear models, with Benjamini–Hochberg correction for multiple testing. For RNA-seq data, raw counts were pre-processed and filtered using edgeR and DESeq2 pipelines. Low-count miRNAs were filtered out prior to normalization using the variance-stabilizing transformation (VST). Principal component analysis (PCA) and heatmaps were used to visualize group clustering. Differential expression analysis between age groups was performed using DESeq2, with an adjusted p -value (FDR) < 0.05 considered significant. Volcano plots were generated using the ggplot2 package. k -means clustering was applied to \log_2 -transformed miRNA expression values using the stats::kmeans function with a fixed number of clusters ($k = 4$), determined by silhouette and elbow methods. Functional enrichment of predicted miRNA targets was conducted using the clusterProfiler package, employing Gene Ontology (GO) and KEGG databases. Enrichment significance was determined by hypergeometric testing with FDR correction. To assess associations between EV characteristics (e.g., particle number/concentration size) and clinical aging markers, Spearman correlation coefficients were computed, and significance was adjusted using the Benjamini–Hochberg method. Spearman correlation analyses between EV features and clinical markers were performed both in the overall cohort and stratified by sex to explore potential sex-specific associations. Heatmaps of correlation matrices were generated using the ComplexHeatmap package. Sex-stratified analyses were also performed to identify sex-specific associations. Finally, linear regression models were used to evaluate associations between individual miRNA expression levels (\log_2 -transformed counts) and biological or functional aging indicators (e.g., GDF-15, grip strength, chair test, visceral fat, and dietary scores). Linear regression models evaluating associations between individual miRNAs and clinical outcomes included chronological age and sex as covariates. Each clinical outcome was modeled separately as: Outcome \sim Age + Sex + miRNA expression. Beta coefficients and p -values were extracted for each miRNA term, and p -values were adjusted for multiple testing using the Benjamini–Hochberg method. This approach was chosen to identify miRNA-phenotype associations independent of chronological age, allowing us to assess whether specific miRNAs associate with biological aging markers beyond their correlation with age itself. For EV characteristic analyses (particle concentration and size), age group (categorical: young, middle-aged, old) and sex were included as independent variables. Spearman correlation analyses between EV features and clinical markers were performed both in the overall cohort and stratified by sex to explore potential sex-specific associations. Due to the limited sample size ($n = 39$, with ≤ 7 individuals per age/sex stratum), we did not adjust for comorbidities or smoking status in our primary analyses. While participants with well-controlled chronic conditions were included, the low frequency of individual comorbidities precluded meaningful adjustment. This represents an important limitation of our study and is discussed in the discussion. Volcano plots were generated to display the strength and significance of miRNA-phenotype associations, with beta coefficients and adjusted p -values from each model. A p -value or FDR < 0.05 was considered statistically significant for all analyses unless otherwise specified.

Data availability

The datasets generated and/or analyzed during the current study are not publicly available due to ethical restrictions related to patient privacy and confidentiality, but are available from the corresponding author on reasonable request. Data are located in controlled access data storage at Health Research Institute of the Balearic Islands (IdISBa).

Code availability

All scripts used for the analysis (preprocessing, differential expression, EV-miRNA quantification, and statistical modeling) are available upon reasonable request from the corresponding author.

Received: 21 May 2025; Accepted: 12 December 2025;

Published online: 14 February 2026

References

- Dziechciaz, M. & Filip, R. Biological psychological and social determinants of old age: bio-psycho-social aspects of human aging. *Ann. Agric Environ. Med.* **21**, 835–838 (2014).
- Kritsilis, M. et al. Ageing, cellular senescence and neurodegenerative disease. *Int. J. Mol. Sci.* **19**, 2937 (2018).
- Polidori, M. C. Aging hallmarks, biomarkers, and clocks for personalized medicine: (re)positioning the limelight. *Free Radic. Biol. Med.* **215**, 48–55 (2024).
- Panagioutou, N., Neytchev, O., Selman, C. & Shiels, P. G. Extracellular vesicles, ageing, and therapeutic interventions. *Cells* **7**, 110 (2018).
- Welsh, J. A. et al. Minimal information for studies of extracellular vesicles (MISEV2023): from basic to advanced approaches. *J. Extracell. Vesicles* **13**, e12404 (2024).
- Manni, G. et al. Extracellular vesicles in aging: an emerging hallmark? *Cells* **12**, 527 (2023).
- O'Brien, K., Breyne, K., Ughetto, S., Laurent, L. C. & Breakefield, X. O. RNA delivery by extracellular vesicles in mammalian cells and its applications. *Nat. Rev. Mol. Cell Biol.* **21**, 585–606 (2020).
- Robbins, P. D. & Morelli, A. E. Regulation of immune responses by extracellular vesicles. *Nat. Rev. Immunol.* **14**, 195–208 (2014).
- Bartel, D. P. MicroRNAs: genomics, biogenesis, mechanism, and function. *Cell* **116**, 281–297 (2004).
- Turchinovich, A., Samatov, T. R., Tonevitsky, A. G. & Burwinkel, B. Circulating miRNAs: Cell-cell communication function? *Front Genet* **4**, 53855 (2013).
- Xu, D. & Tahara, H. The role of exosomes and microRNAs in senescence and aging. *Adv. Drug Deliv. Rev.* **65**, 368–375 (2013).
- Yamamoto, T., Kosaka, N., Hattori, Y. & Ochiya, T. A Challenge to aging society by microRNA in extracellular vesicles: microRNA in extracellular vesicles as promising biomarkers and novel therapeutic targets in multiple myeloma. *J. Clin. Med.* **7**, 55 (2018).
- Xiao, X. et al. Mesenchymal stem cell-derived small extracellular vesicles mitigate oxidative stress-induced senescence in endothelial cells via regulation of miR-146a/Src. *Signal. Transduct. Target Ther.* **6**, 354 (2021).
- Yang, X. et al. Endothelial cell-derived extracellular vesicles target TLR4 via miRNA-326-3p to regulate skin fibroblasts senescence. *J. Immunol. Res.* **2022**, 3371982 (2022).
- Hu, L. et al. MiR-1224-5p modulates osteogenesis by coordinating osteoblast/osteoclast differentiation via the Rap1 signaling target ADCY2. *Exp. Mol. Med.* **54**, 961–972 (2022).
- Heid, J. et al. Age-dependent increase of oxidative stress regulates microRNA-29 family preserving cardiac health. *Sci. Rep.* **7**, 16839 (2017).
- Cechinel, L. R. et al. Circulating total extracellular vesicles cargo are associated with age-related oxidative stress and susceptibility to cardiovascular diseases: exploratory results from microarray data. *Biomedicines* **11**, 2920 (2023).
- Tsukamoto, H., Kouwaki, T. & Oshiumi, H. Aging-associated extracellular vesicles contain immune regulatory microRNAs alleviating hyperinflammatory state and immune dysfunction in the elderly. *iScience* **23**, 101520 (2020).
- Mas-Bargues, C. & Alique, M. Extracellular vesicles as “Very Important Particles” (VIPs) in aging. *Int. J. Mol. Sci.* **24**, 4250 (2023).
- Yin, Y., Chen, H., Wang, Y., Zhang, L. & Wang, X. Roles of extracellular vesicles in the aging microenvironment and age-related diseases. *J. Extracell. Vesicles* **10**, e12154 (2021).
- Sanz-Ros, J. et al. Therapeutic potential of extracellular vesicles in aging and age-related diseases. *Int. J. Mol. Sci.* **23**, 14632 (2022).
- Robbins, P. D. Extracellular vesicles and aging. *Stem Cell Investig.* **4**, 98 (2017).
- Borras, C. et al. Extracellular vesicles and redox modulation in aging. *Free Radic. Biol. Med.* **149**, 44–50 (2020).
- Noren Hooten, N. Extracellular vesicles and extracellular RNA in aging and age-related disease. *Transl. Med. Aging* **4**, 96–98 (2020).
- Alibhai, F. J. et al. Cellular senescence contributes to age-dependent changes in circulating extracellular vesicle cargo and function. *Aging Cell* **19**, e13103 (2020).
- Torrens, M. et al. GDF-15 as a proxy for epigenetic aging: associations with biological age markers, and physical function. *Biogerontology* **26**, 22 (2024).
- Tanaka T. et al. Plasma proteomic signature of age in healthy humans. *Aging Cell* **17**, e12799 (2018).
- Eitan, E. et al. Age-related changes in plasma extracellular vesicle characteristics and internalization by leukocytes. *Sci. Rep.* **7**, 1342 (2017).
- Zhang, X. et al. Immune system-related plasma extracellular vesicles in healthy aging. *Front. Immunol.* **15**, 1355380 (2024).
- Holcar, M. et al. Comprehensive phenotyping of extracellular vesicles in plasma of healthy humans—insights into cellular origin and biological variation. *J. Extracell. Vesicles* **14**, e70039 (2025).
- Burrello, J. et al. Age- and sex-related variations in extracellular vesicle profiling for the assessment of cardiovascular risk: the EVaging index. *NPJ Aging* **10**, 63 (2024).
- Mulcahy L. A., Pink R. C. & Carter D. R. Routes and mechanisms of extracellular vesicle uptake. *J. Extracell. Vesicles* **3**, <https://doi.org/10.3402/jev.v3.24641> (2014).
- Kern, F. et al. Ageing-associated small RNA cargo of extracellular vesicles. *RNA Biol.* **20**, 482–494 (2023).
- Jie, R. et al. Role of increased miR-222-3p expression in peripheral blood and wound marginal tissues of type 2 diabetes mellitus patients with diabetic foot ulcer. *Diab. Metab. Syndr. Obes.* **16**, 2419–2432 (2023).
- Dégano I. R. et al. Association of circulating microRNAs with coronary artery disease and usefulness for reclassification of healthy individuals: The REGICOR Study. *J. Clin. Med.* **9**, 1402 (2020).
- Chistiakov D. A., Sobenin I. A., Orekhov A. N. & Bobryshev Y. V. Human miR-221/222 in physiological and atherosclerotic vascular remodeling. *Biomed. Res. Int.* 354517, <https://doi.org/10.1155/2015/354517> (2015).
- Dentelli, P. et al. microRNA-222 controls neovascularization by regulating signal transducer and activator of transcription 5A expression. *Arterioscler. Thromb. Vasc. Biol.* **30**, 1562–1568 (2010).
- Ma, G. et al. MiR-206, a key modulator of skeletal muscle development and disease. *Int. J. Biol. Sci.* **11**, 345–352 (2015).
- Liu, N. et al. microRNA-206 promotes skeletal muscle regeneration and delays progression of Duchenne muscular dystrophy in mice. *J. Clin. Invest.* **122**, 2054–2065, (2012).
- He, N. et al. Circulating microRNAs in plasma decrease in response to sarcopenia in the elderly. *Front. Genet.* **11**, 167 (2020).
- Yamaura, Y., Kanki, M., Sasaki, D., Nakajima, M. & Unami, A. Serum miR-206 as a biomarker for drug-induced skeletal muscle injury in rats. *J. Toxicol. Sci.* **45**, 503–513 (2020).
- Soriano-Arroquia, A., McCormick, R., Molloy, A. P., McArdle, A. & Goljanek-Whysall, K. Age-related changes in miR-143-3p:lgbp5 interactions affect muscle regeneration. *Aging Cell* **15**, 361–369 (2016).
- Xihua, L. et al. Circulating miR-143-3p inhibition protects against insulin resistance in Metabolic Syndrome via targeting of the insulin-like growth factor 2 receptor. *Transl. Res.* **205**, 33–43 (2019).

44. Nasi, V. L. et al. miR-21-5p regulates mitochondrial respiration and lipid content in H9C2 cells. *Am. J. Physiol. Heart Circ. Physiol.* **316**, H710–H721 (2019).
45. Lin, K. et al. Plasma exosomal miRNA expression and gut microbiota dysbiosis are associated with cognitive impairment in Alzheimer's disease. *Front Neurosci.* **19**, 1545690 (2025).
46. Slack, C. Ras signaling in aging and metabolic regulation. *Nutr. Healthy Aging* **4**, 195–205 (2017).
47. Grunewald, M. et al. Counteracting age-related VEGF signaling insufficiency promotes healthy aging and extends life span. *Science* **373**, eabc8479 (2021).
48. Paganelli, R. et al. A shift to Th0 cytokine production by CD4+ cells in human longevity: studies on two healthy centenarians. *Eur. J. Immunol.* **26**, 2030–2034 (1996).
49. Audunsdottir, K. & Quintana, D. S. Oxytocin's dynamic role across the lifespan. *Aging Brain* **2**, 100028 (2022).
50. Franceschi, C. et al. Inflamm-aging. An evolutionary perspective on immunosenescence. *Ann. N. Y Acad. Sci.* **908**, 244–254 (2000).
51. Duffy, J. F., Zitting, K. M. & Chinoy, E. D. Aging and Circadian Rhythms. *Sleep. Med. Clin.* **10**, 423–434 (2015).
52. Volkow, N. D. et al. Association between decline in brain dopamine activity with age and cognitive and motor impairment in healthy individuals. *Am. J. Psychiatry* **155**, 344–349 (1998).
53. Visconte, C. et al. Plasma microglial-derived extracellular vesicles are increased in frail patients with mild cognitive impairment and exert a neurotoxic effect. *Geroscience* **45**, 1557–1571 (2023).
54. Romero-García, N. et al. The double-edged role of extracellular vesicles in the hallmarks of aging. *Biomolecules* **13**, 165 (2023).
55. Terlecki-Zaniewicz, L. et al. Extracellular vesicles in human skin: cross-talk from senescent fibroblasts to keratinocytes by miRNAs. *J. Investig. Dermatol.* **139**, 2425–2436.e5 (2019).
56. Conkright, W. R. et al. Resistance exercise differentially alters extracellular vesicle size and subpopulation characteristics in healthy men and women: an observational cohort study. *Physiol. Genomics* **54**, 350–359 (2022).
57. Norman K., Stobäus N., Pirlich M. & Bösly-Westphal A. Bioelectrical phase angle and impedance vector analysis—clinical relevance and applicability of impedance parameters. *Clin Nutr.* **31**, 854–861 (2012).
58. Wilhelm-Leen E. R., Hall Y. N., Horwitz R. I. & Chertow G. M. Phase angle, frailty and mortality in older adults. *J. Gen. Intern. Med.* **29**, 147–154 (2014).

Acknowledgements

This work was supported by the Instituto de Salud Carlos III (ISCIII) (Miguel Servet Program-MS19/00201, and PI21/01480), Ministerio de Ciencia, Innovación y Universidades (Agencia Española de Investigación (AEI), CNS2022-135110), and the Impost turisme sostenible/Govern de les Illes Balears (FOLIUM program—19/01 and SYNERGIA program SYN22/04). We gratefully acknowledge the essential contributions of the Clinical Unit of the Research Institute of the Balearic Islands, the Biobank Unit, and the Hospital

Universitario Son Espases for their support in data collection. We are especially thankful to all the participants who generously contributed to this study. We also acknowledge Novogene (UK) Company Limited for their sequencing services. We would like to thank Anna Estela Bolta, PhD, Senior Account Manager (Novogene, UK), for her support and assistance throughout the project.

Author contributions

C.R.-M., J.M.R., M.M., X.C., M.T.-M., C.N.-E., and M.G.-F. were involved in the study conception, design, and experimental protocol; C.R.-M., J.M.R., X.C., A.M.G.-P., C.N.-E., L.M., M.T.-M., A.S.P., A.M.-L., M.M.-C., A.B.-A., J.M.R., and M.G.-F. collected the data and helped with the data analysis. C.R.-M., C.N.-E., M.T.-M., X.C., J.M.R., and M.G.-F. analyzed the data and wrote the manuscript. All authors have read and agreed to the published version of the manuscript.

Competing interests

The authors declare no competing interests.

Additional information

Supplementary information The online version contains supplementary material available at <https://doi.org/10.1038/s41514-025-00321-1>.

Correspondence and requests for materials should be addressed to JM Ramis or M. Gonzalez-Freire.

Reprints and permissions information is available at <http://www.nature.com/reprints>

Publisher's note Springer Nature remains neutral with regard to jurisdictional claims in published maps and institutional affiliations.

Open Access This article is licensed under a Creative Commons Attribution-NonCommercial-NoDerivatives 4.0 International License, which permits any non-commercial use, sharing, distribution and reproduction in any medium or format, as long as you give appropriate credit to the original author(s) and the source, provide a link to the Creative Commons licence, and indicate if you modified the licensed material. You do not have permission under this licence to share adapted material derived from this article or parts of it. The images or other third party material in this article are included in the article's Creative Commons licence, unless indicated otherwise in a credit line to the material. If material is not included in the article's Creative Commons licence and your intended use is not permitted by statutory regulation or exceeds the permitted use, you will need to obtain permission directly from the copyright holder. To view a copy of this licence, visit <http://creativecommons.org/licenses/by-nc-nd/4.0/>.

© The Author(s) 2026